

International Conference on Space Optics—ICSO 2014

La Caleta, Tenerife, Canary Islands

7–10 October 2014

Edited by Zoran Sodnik, Bruno Cugny, and Nikos Karafolas



Overview on grating developments at ESA

B. Guldemann

A. Deep

R. Vink

B. Harnisch

et al.



OVERVIEW ON GRATING DEVELOPMENTS AT ESA

B. Guldemann, A. Deep, R. Vink, B. Harnisch, S. Kraft, B. Sierk, G. Bazalgette, J.-L. Bézy
ESA-ESTEC, Keplerlaan 1, NL - 2200 AG Noordwijk, The Netherlands.

1) INTRODUCTION

In the frame of recent studies and missions, ESA has been performing various pre-developments of optical gratings for instruments operating at wavelengths from the UV up to the SWIR. The instrument requirements of Sentinel-4, Sentinel-5, CarbonSat and FLEX are driving the need for advanced designs and technologies leading to gratings with high efficiency, high spectral resolution, low stray light and low polarization sensitivities. Typical ESA instruments (e.g. Sciamachy, GOME, MERIS, OLCI, NIRSpec) were and are based on ruled gratings or gratings manufactured with one holographic photoresist mask layer which is transferred to an optical substrate (e.g. glass, glass ceramic) with dry etching methods and subsequently either coated with a reflective coating or used as a mold for replication. These manufacturing methods lead to blazed grating profiles with a metallic reflective surface. The vast majority of spectrometers on ground are still based on such gratings. In general, gratings based on grooved metallic surfaces tend for instance to polarize the incoming light significantly and are therefore not always suitable for ESA's needs of today. Gratings made for space therefore evolved to many other designs and concepts which will be reported in this paper.

2) OVERVIEW ON THE MAIN GRATING MANUFACTURING TECHNIQUES

All grating developments initiated by or for ESA in the past years have been manufactured using reactive ion beam etching [1]. The difference leading to application specific grating designs and concepts were essentially the shape of the grating substrates and the technology used to generate the etch mask. Ruled gratings are not manufactured for ESA in Europe anymore since over 5 years, the last being the grating for NIRSpec. This chapter introduces the most common etch mask manufacturing techniques recently used.

Holographic etch mask

The fact that holograms can be produced also on non-planar surfaces and can be recorded on substrates of any thickness, makes this masking method indispensable. The effort to obtain an accurate and repeatable holographic etch mask, increases with the grating size, the required quality of the wave front and efficiency. Assuming a repeatable etching process, the main challenges to obtain the designed grating profile are a repeatable exposure, development, curing and storage of the photoresist layer before it is used in the etcher. The blaze angle and other detailed profile design parameters can easily vary from one manufactured grating to the next due for instance to slight variations in the processing of the substrates (e.g. priming) and photoresist layer (e.g. spin coating, exposure, development, curing and storage time and conditions). The etch process transferring the grating profile recorded in the photoresist into the substrate is not trivial since the recorded 3D profile in the photoresist is usually not transferred one to one into the substrate. Depending on the photoresist and the substrate material, the depth of the transferred/etched profile can be for instance 6 times the structure height of the photo resist profile (mask selectivity of 6). Selectivity, or transfer factors, can be tailored by the manufacturer. At a more detailed level, the etch rate depends also on the etch process, instantaneous shape of the photoresist mask and instantaneous groove geometry (e.g. aspect ratio = groove depth/ groove width). One of the simplest photoresist mask profiles to be produced using holography is of a sinusoidal shape. With particular asymmetric illumination conditions, asymmetric profiles (e.g. blaze) can be obtained. Despite inherent limitations of holographic exposure for obtaining arbitrary profiles, an impressive range of groove profile geometries are possible (fig. 1). Since the manufacturing of holographic masks is usually not dependent on any mechanical stepping tools, unlike the lithographic etch masks or ruling engines, they do not generate ghosts.

To summarize, gratings profiles generated from holographic etch masks have no ghosts (assuming adequate holographic exposure) and can be manufactured on non-flat and thick substrates. They need however an extra development effort for optimizing the manufacturing processes for each new grating design.

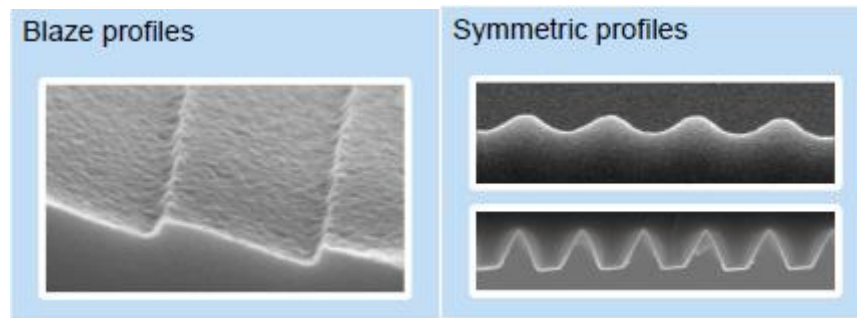


Fig. 1: Examples of grating profiles produced by ZEISS in Jena with holographic etch mask

Lithographic etch mask

Micro-electronic circuit manufacturing and development tools have reached a level where large (up to diameters of 30 cm) planar photoresist layers can be patterned with very high resolution and accuracy [2]. It is therefore possible to manufacture large gratings without compromising on the wave front error. Particularly relevant for grating manufacturing, these lithography tools (e.g. photo-lithography, e-beam lithography) are complemented by MEMS manufacturing tools for deep trenching silicon or other materials (e.g. glass, ceramic) and alignment-bonders for bonding prisms to planar grating substrates for instance. Such “tool parks” combined with the availability of a wide range of photo-resists as well as novel coating technologies extends significantly the available grating design parameters as well as options for optimizing the manufacturing processes. An elegant example showing some of the new possibilities and advantages offered by these tools and associated expertise is the grating produced by Fraunhofer IOF in Jena for the GAIA project [3] (fig. 2). It is elegant, because a very large grating has been produced with a standard planar mask pattern and a single etch step leading to a binary profile mimicking a blazed grating. And it offers new possibilities, because it broke through the inherent limitations of all existing grating manufacturing technologies and in particular the ability to achieve accurate patterning in the cross dispersion direction.

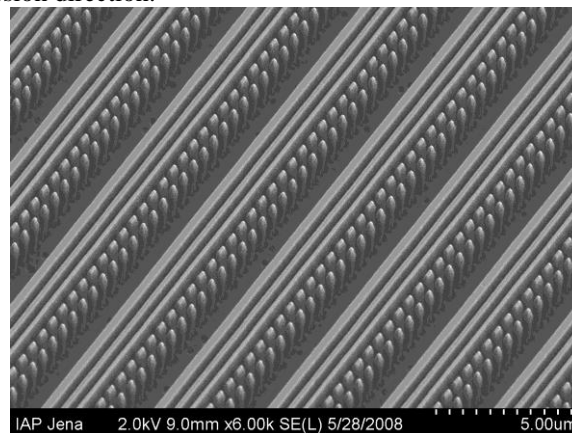


Fig. 2: SEM picture of the GAIA grating manufactured at Fraunhofer IOF in Jena

The advantage of gratings based on binary profiles generated by lithographic methods, is the simplicity of the etch mask (planar) which simplifies a standardization of the manufacturing of the mask as well as of the etching process for the production of the grooves. Binary gratings have the advantage that a well-known set of parameters are available for designing the profile, namely the depth and the width(s) of the groove(s) for each period. Due to the simplicity of the profile geometry, these design parameters can describe the manufactured grating profile accurately enough to predict the optical performances. A limitation so far has been however the generation of spectral and spatial ghosts (side peaks in the BSDF response) due to artifacts from the step-write process of the e-beam writers. The e-beam writes a limited, relatively small area in one scan. Then it has to move the substrate to the next writing area with a mechanism, introducing a small stitching error. This leads to slight periodic misalignments in the grating profile. Very recently, techniques are becoming available to reduce those ghosts. A practical limitation to this manufacturing method is usually the thickness of the substrate, since the tools used for MEMS or micro-electronics manufacturing are optimized for plane and relatively thin substrates.

To summarize, gratings generated by lithographic e-beam masks have the advantage to generate arbitrary 2D or, by using multi-layered etching, arbitrary 3D profiles, and to use very predictable and repeatable manufacturing processes within a large flat surface area. The main remaining disadvantage of this method are the ghosts, but there are techniques to reduce them if the application requires it.

3) OVERVIEW OF RECENT ESA GRATING PRE-DEVELOPMENTS

NIR immersed grating

In the frame of an ESA TRP contract (#23122) SSTL and Horiba Jobin Yvon have developed an immersed grating for high spectral resolution spectroscopy for operation in the NIR typically applicable to Earth observation missions. For any required spectral dispersion value, immersed gratings [4] have by a factor n ($n_i =$ refractive index of the immersion medium / substrate) reduced length compared to other grating concepts. This leads to a smaller spectrometer collimator and camera diameters and therefore to a volume reduction of up to a factor n_i^3 . Horiba Jobin Yvon manufactured a binary grating profile (fig. 3) using a holographic etch mask which was transferred with ion beam etching to a flat fused silica substrate. The diffractive layer profile is designed for obtaining one order of diffraction in reflection back to the fused silica only. No reflective coating is therefore required. The $120 \times 120 \text{ mm}^2$ grating substrate was then optically contact bonded to a (fused silica?) prism, optically characterized and passed the thermal vacuum tests.

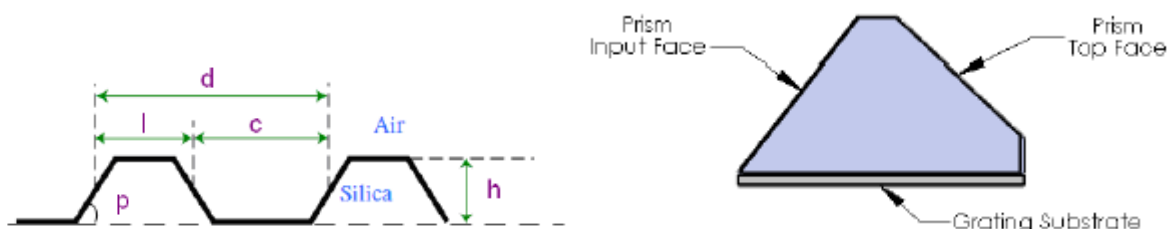


Fig. 3: Profile of the fused silica immersed grating and complete immersed grating after optical contacting. The profile parameters are: $h=450\text{nm}$, $d=310\text{nm}$ ($N=3226 \text{ l/mm}$), duty cycle $c/d=0.6$, slope $p=85^\circ$. The grating length is 110 mm .

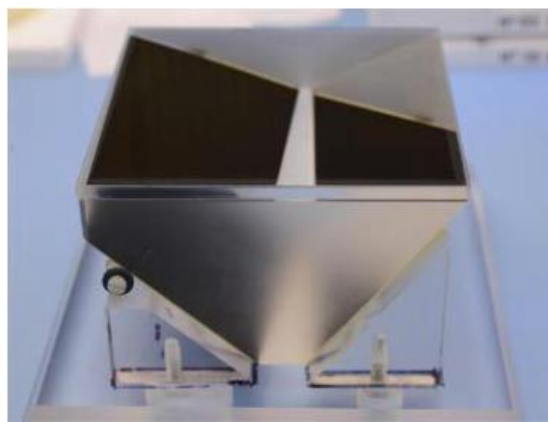


Fig. 4: The completed NIR immersed grating (photo courtesy of SSTL)

Sentinel-4 UV-VIS and NIR gratings

Sentinel-4 is an atmospheric chemistry instrument operating from geostationary orbit planned to be embarked on the Meteosat Third Generation sounding satellites. The instrument concept is based on dispersive imaging spectrometers. Its optical design is based on refractive optics in order to minimize polarization sensitivity. One of the very few reflective optical elements is the NIR grating. The NIR grating was designed to operate in reflection enabling a double pass spectrometer optical design which minimizes volume and mass. Some of the particular specifications of the Sentinel 4 instrument driving its design and grating requirements (Table 1) are for instance low straylight and low polarisation sensitivity. Furthermore the amplitude of spurious spectral features needs to be minimised as they could correlate with the spectral structure of the atmospheric absorbing molecular species. This NIR grating of Sentinel-4 (fig. 5) is the second good example of how micro-technologies can be spun in for manufacturing new types of gratings. Fraunhofer Institute of IOF-Jena designed a grating using an embedded reflective multilayer coating which serves as highly reflective broadband surface as well as a reducer of polarizations sensitivity. On top of this reflective coating a silicon dioxide layer is deposited which is then etched to form the binary diffractive profile. The incident beam is diffracted twice in fact, the first time entering the profiled dioxide layer from vacuum/air and a second time after reflection from the multilayer coating leaving the dioxide layer. Stray light levels measured on a representative reduced size sample were at an equivalent level to a mirror surface with 3nm RMS micro-roughness. The specifications of

the pre-developed NIR grating are summarised in Table 1. The measured efficiency of the zeroth order is shown in Fig. 6. The NIR grating is now following the full development to a flight model.

Tab. 1: Sentinel-4 diffraction gratings specifications

	Unit	S4 UV-VIS	S4 NIR
Grating type		3-layered blazed in transmission	binary, in reflection with embedded multilayer coating
Wavelength range	nm	305 – 500	750-775
Used diffraction order	-	-1	-1
Line density	l/mm	528	1,255
Grating period	nm	1894	797
Dent width	nm	3-layer blazed	477
Groove width	nm	1694	390
Groove depth	nm	486	782
Aspect ratio		0.3	2.0
Angle of incidence	deg	15.636° (in SiO ₂) 23.6° (in air)	37.7°
Diffraction efficiency target		50%	>70%
Polarization sensitivity		<2%	<4%
Polarization dependent spectral features		<0.15% (in spectral window of 3nm) <5% (in spectral window of 100nm)	<0.8% (in spectral window of 7.5nm) <5% (in spectral window of 25nm)
Substrate material		fused silica	fused silica multilayer coated with coated SiO ₂ top layer for the grooves
Grating size	mm	68 x 68	elliptical 56x60
Development status		Reduced size (30x30mm ²) manufactured	Reduced size (30x30mm ²) manufactured Now in process to become fully space qualified

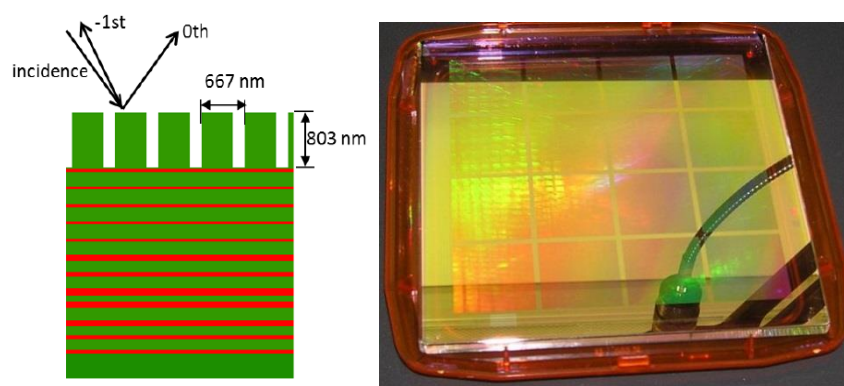


Fig. 5: The picture on the left shows the S4 NIR grating profile with its embedded high reflective coating and the photo on the right are the pre-developed samples on a large fused silica substrate. (photo courtesy of IOF)

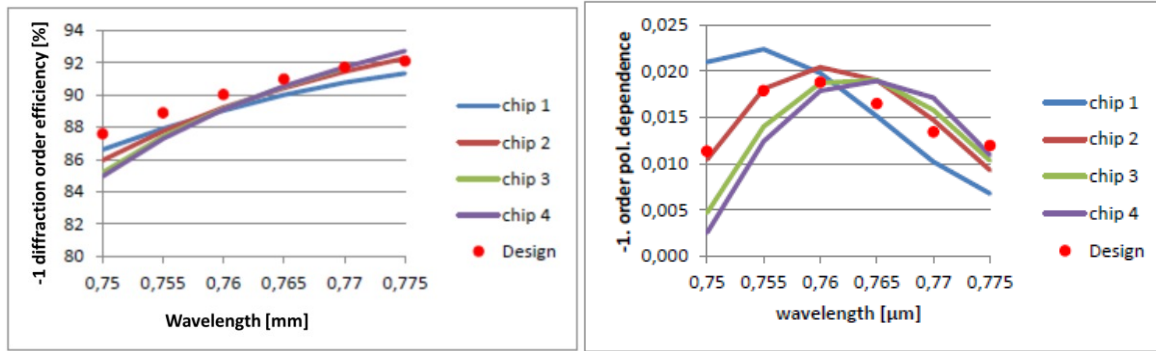


Fig. 6: -1st order efficiency (TE) and polarisation sensitivity. The -1st order being close to the Littrow angle, its efficiency can in practice not be measured directly. It was derived from the zeroth-order efficiency measurement.

The UV-VIS spectrometer of Sentinel-4 is a fully refractive instrument based on a grism with an operational wavelength range from 305nm to 500nm. The grism has been pre-developed in an early phase of the Sentinel-4 project by IOF and was based on a multilayer blazed grating design (fig. 7). The pre-developed gratings were characterized without the prism bonded to the grating (fig. 8).

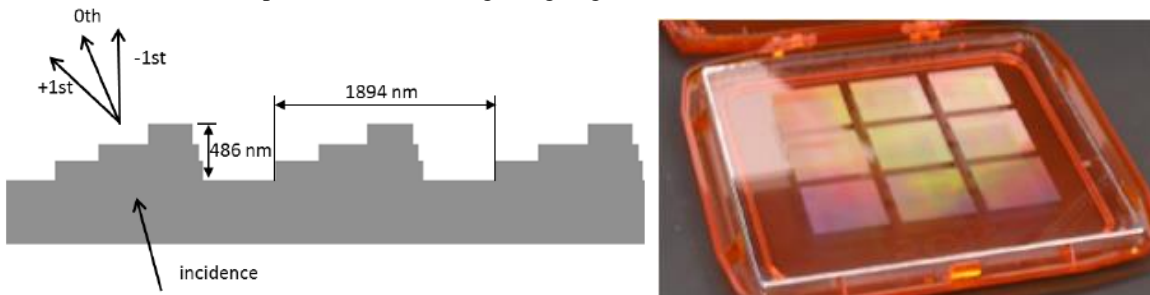


Fig. 7: On the left the Sentinel-4 UV-VIS grism profile is shown and on the right a photograph of the 9 pre-developed grating samples on a large substrate can be seen. (photo courtesy of IOF)

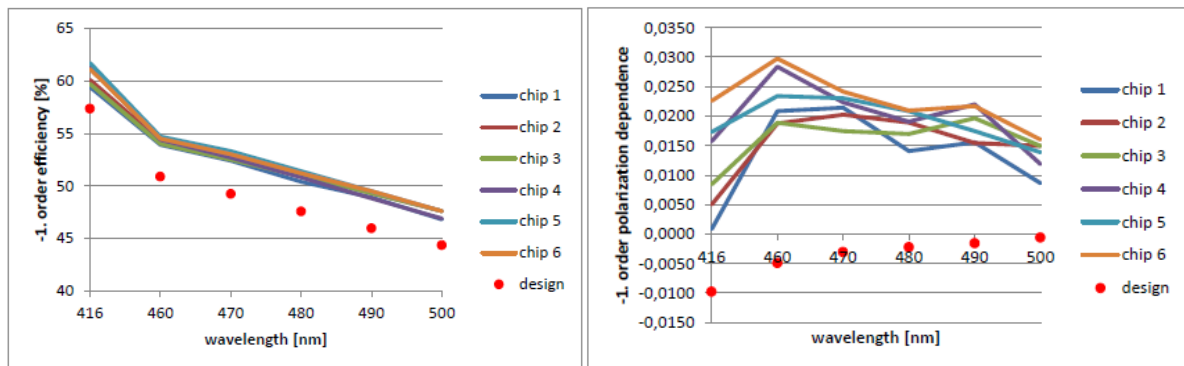


Fig. 8: on the left the -1st order efficiencies and on the right the polarization sensitivities of the pre-developed S4 UV-VIS grating are shown. Those performances met the requirements of Sentinel-4.

Sentinel 5 grating pre-developments

Sentinel-5 is an atmospheric chemistry instrument planned to be embarked on the MetOp Second Generation satellites. Similarly to sentinel-4, the instrument concept is based on dispersive imaging spectrometers. In the frame of the Sentinel-5 ESA phase A/B1 two competing prime contractors, Airbus Defense & Space (ADS) and Kayser-Threde (KT, part of OHB), initiated grating pre-developments for some of the spectrometer channels.

Grating pre-developments of KT

Tab. 2 summarizes the grating specifications of the pre-developments made in the frame of the Sentinel-5 study by KT for the UV (270nm-380nm), VIS (370nm-500nm) and NIR (755nm-773nm) spectrometers.. The UV channel design was based on an Offner spectrometer with a convex blazed grating (fig. 9). The grating pre-developed at ZEISS in Jena focused on two main manufacturing steps, first the creation of a grating structure in a photo resist layer covering the fused silica grating substrate blank by holographic exposure, followed by the transfer of the structured resist into the substrate by reactive ion beam etching. At the end the grating was coated

with aluminum. One of the challenges with this curved grating is to manufacture the local blaze angle constant with respect to the local normal surface over the whole illuminated area.

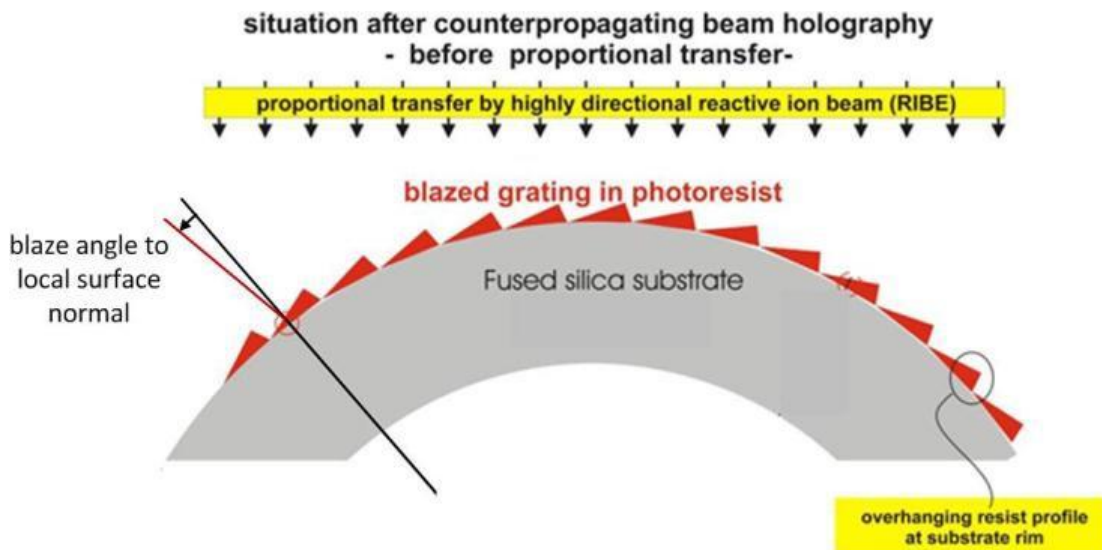


Fig. 9: Proportional transfer by reactive ion beam etching on a convex substrate, here with exaggerated geometries. (image courtesy of ZEISS)

The grating performances and specifications are summarized in Table 2. Surface roughness, relevant for stray light performance, has been measured with an AFM. The RMS roughness was calculated by subtracting the linear slope and subsequently taking the standard deviation results for four grating samples. This gave an average value slightly above 4 nm RMS. It must be noted that an AFM measurements encompasses also spatial frequencies which are not very relevant for the generation of straylight and that an optical measurement of the roughness would be more adequate. Straylight measurements have also been performed (fig. 10) by ZEISS as well as successful thermal vacuum tests.

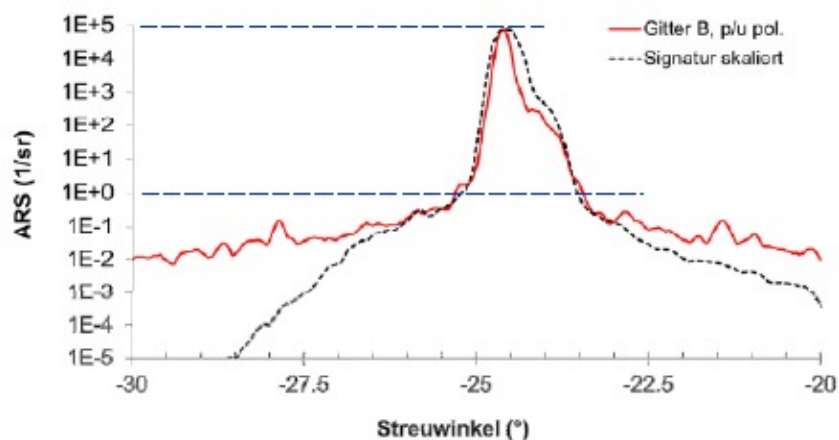


Fig. 10: Straylight measurement result of the convex UV grating for the Sentinel-5 study of KT

Tab. 2: Specifications of the pre-developed Sentinel-5 gratings (by KT)

	Unit	UV	VIS	NIR
Manufacturer		ZEISS	IOF	IOF
Grating type		reflective convex blazed spherical surface radius of 237 mm	binary transmission	Binary transmission
Etch mask		Holographic, counter propagating	e-beam lithographic	e-beam lithographic
Wavelength range	nm	270 - 380	370 - 500	755-773
Used diffraction order	-	-1	-1	-1
Line density	l/mm	907.3	2463	2267
Grating period	nm	1102	406	441
Dent width	nm	NA (blazed ~11°)	252	149
Groove width	nm	NA (blazed ~11°)	154	292
Groove depth	nm	180	950	956
Trench aspect ratio width/depth		NA	3.8	3.3
Angle of incidence	deg	50	19.1 (in substrate)	38.1 (in substrate)
Diffraction efficiency target		>60%	>63%	>85%
Polarization sensitivity		up to 15%	<5%	<5%
Substrate material		fused silica	fused silica	fused silica
over-Coating		aluminium	NA	Grooves filled with high refractive index material (TiO ₂), then covered with TaO ₅ layer and a SiO ₂ top layer
Grating size	mm	Ø 62 mm	Ø 22 mm	Ø 39 mm
Development status		Full size, manufactured	9 samples, size (30x30mm ²) manufactured	9 reduced size samples (30x30mm ²) manufactured
Qualification status		Thermal vacuum and adherence tests passed	Thermal vacuum and adherence tests passed	Thermal vacuum and adherence tests passed

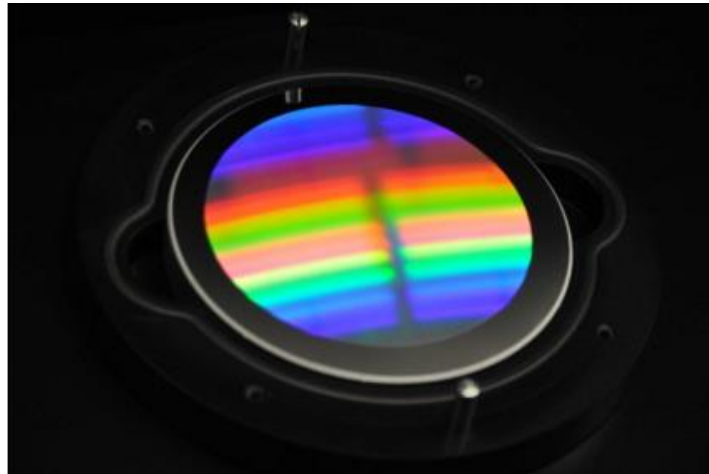


Fig. 11: Manufactured convex UV grating for Sentinel-5 study of KT. (Photo courtesy of ZEISS)

The VIS spectrometer design of KT was based on a transmission grating ($\lambda = 370\text{-}500\text{ nm}$). KT selected a prism grating plus prism configuration (PG+P), as shown in fig. 12, using the first diffraction order in Littrow condition and fused silica as substrates. If the technology were available, the preferred design would have been a PGP configuration, avoiding the air gap between the grating and the second prism. One of the reasons for initially targeting this particular PGP configuration is to reduce volume and mass. Such a grating can also be described as an immersed grating in transmission and has the same volume saving advantage.

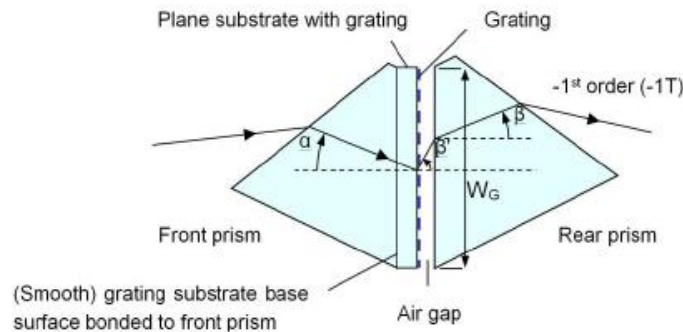


Fig. 12: The prism-grating plus prism design for the VIS channel of the Sentinel-5 study of KT

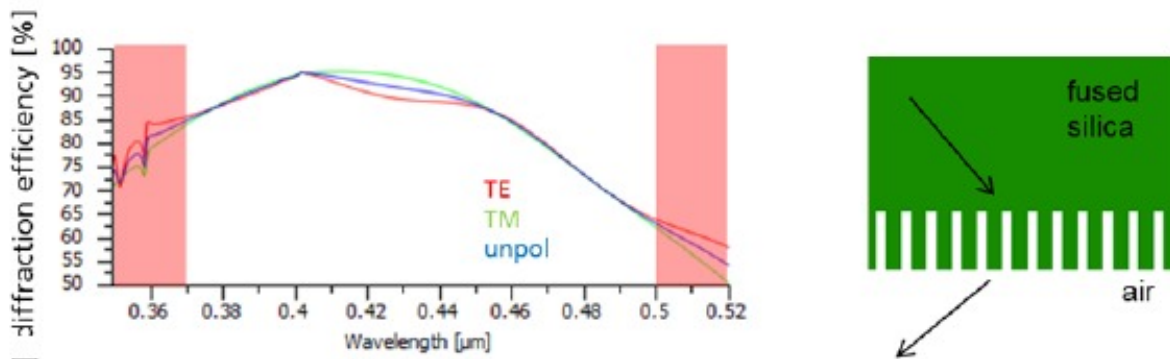


Figure 13: Efficiency and profile of the VIS grating for Sentinel-5 of KT

A binary profile was designed having the calculated efficiencies shown in fig. 13. This pre-development was performed at IOF with the typical e-beam based manufacturing flow diagram shown in fig. 14. The specifications and achieved performances are summarized in Table 2. The aspect ratio of the groove (groove width / groove depth) is about 3.8 and therefore well within today's glass etching capabilities at IOF.

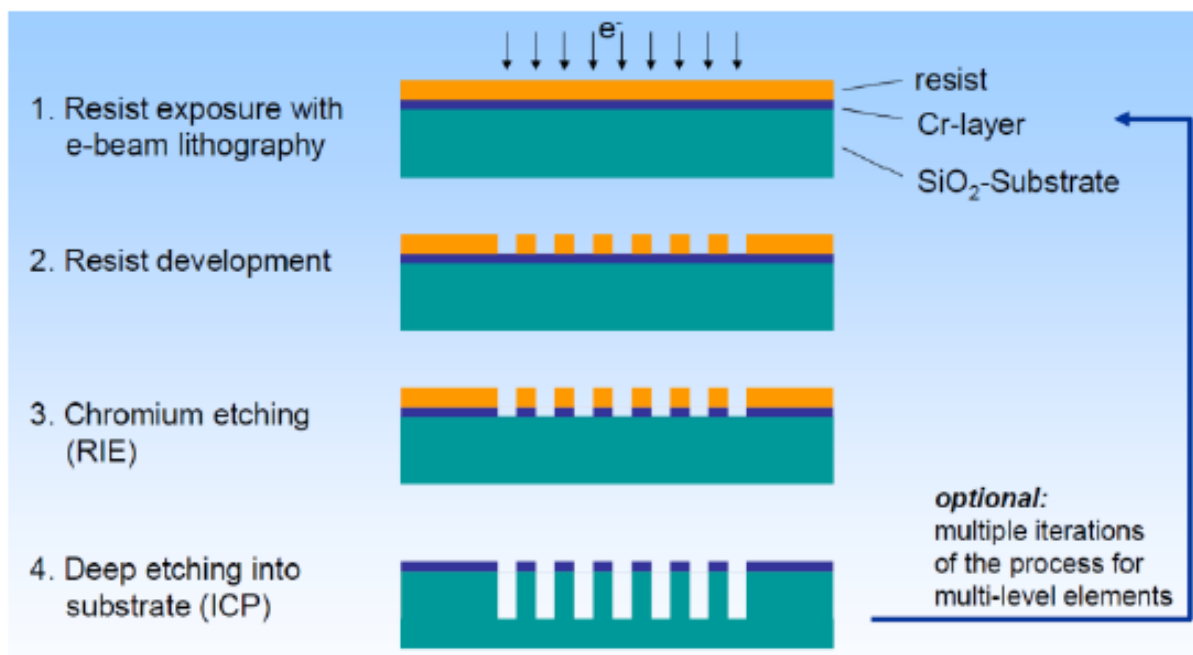


Figure 14: Basic process flow chart for manufacturing gratings with e-beam lithography

Stray-light measurements have been performed at ESA and the results compared to the stray light generated by two mirrors with different surface roughness (fig. 15). The stray light response at scatter angles below 1° shows noticeable side peaks. The strongest side peak is due to multiple reflections inside the substrate. The other peaks are most probably ghosts generated by the e-beam lithographic manufacturing process. For larger angles the stray-light level of the VIS grating is between both reference mirrors. Theory [5] predicts that reflective rough surfaces, for instance mirrors, generate a total integrated scattered (TIS) light level proportional to:

$$\text{TIS}_m \sim (2\sigma_m/\lambda)^2 \quad (1)$$

and for refractive rough surfaces a TIS proportional to

$$\text{TIS}_g \sim ((n_g-1)\sigma_g/\lambda)^2 \quad (2)$$

where n_g is the refractive index of the substrate used. For visible light this means that the total integrated scattered light (TIS) levels generated per reflective surface is 19 times larger than the TIS for a bare transmissive fused silica surface. In this discussion the simplified assumption is made that the scattering of etched grating surfaces can also be described by these TIS equations. Transmission gratings having two rough surfaces contributing to scattered light would, according to this theory, still have an order of magnitude less stray light than a reflective grating/surface with the same roughness. It can therefore be assumed that the effective surface roughness of the transmission grating as reported in fig. 15 has a higher estimated roughness than the 2.7 nm RMS of the reference mirror. The origin of the higher estimated roughness of the transmission grating is most likely the larger roughness of the surfaces machined with the etching process. Assuming that the etched side of the grating substrate is the clearly dominant contributor to scattered light (assuming that the blank substrate was super polished) the roughness of the grating profile may be expressed with:

$$\sigma_g = 2\sigma_m/(n_g-1) \quad (3)$$

leading to a 11 nm RMS estimated value for the fused silica VIS grating diffractive surface. In the overall stray light response contamination also plays a role and direct derivation of the grating surface roughness from stray light measurements is not straightforward.

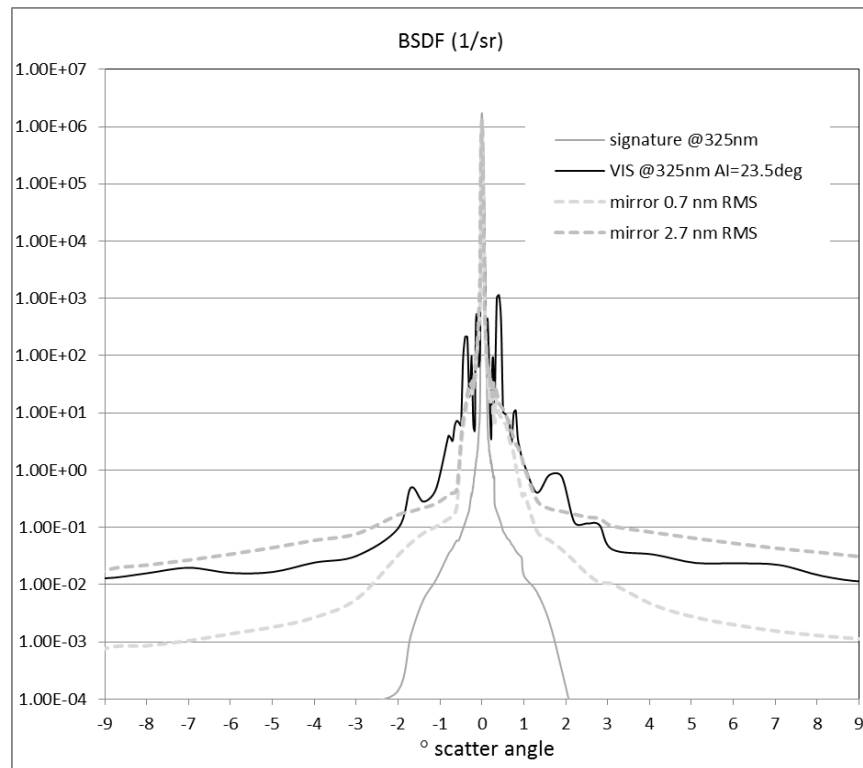


Figure 15: BSDLs at 325nm of the VIS grating of KT and two reference mirrors.

The NIR spectrometer design of KT was similar to the VIS spectrometer with a prism grating plus prism dispersive element (fig. 12) operating in transmission. The grating profile manufactured at IOF using e-beam lithographic etch mask is shown in fig. 16. Its trapezoidal shape was necessary for a successful filling of the grooves with a high refractive index material. Such a high index material was necessary from a design point of view because a diffraction profile based only on fused silica leads to a too large and therefore today unfeasible groove aspect ratio (groove depth / groove width). The additional top bi-layer coating of TaO₅ and SiO₂ were mainly deposited to improve the performances with respect to polarization sensitivity. The efficiencies obtained and calculated are shown in fig. 17. The reason for the lower measured efficiency is attributed to the TaO₅ layer which might absorb more than expected. The measured stray light levels at 633 nm, which is outside the operational spectral range, is shown in fig. 18. At scatter angles below 1° the BSDL has a value less than 1, which is, compared to the diffracted light at a level above 10⁶, quite good. However, up to 1° clear oscillations can be observed, as for the VIS grating. One of the side peaks has amplitude of three orders of magnitude above 1 and could be due to multiple reflections inside the substrate. At scatter angles greater than 3° the scattered light is eight orders of magnitude lower than the diffraction order.

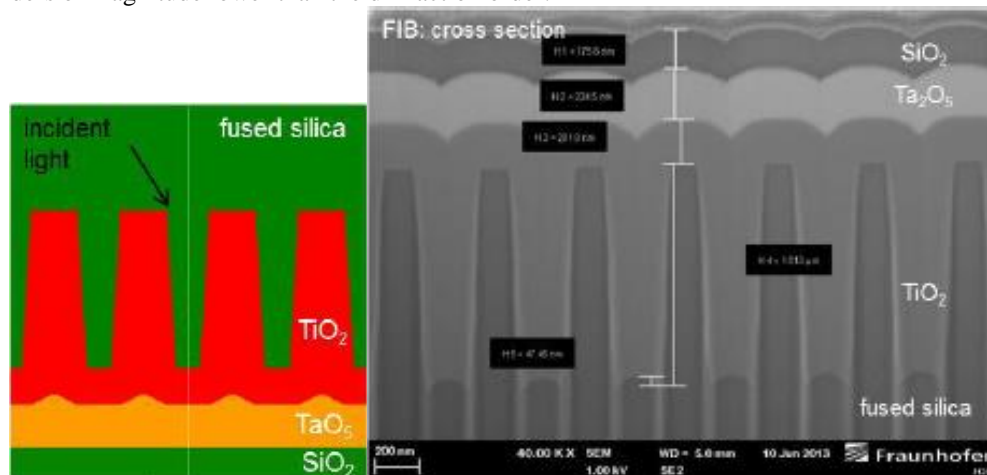


Fig. 16: On the left a drawing of the NIR grating profile and on the right an SEM picture of the cross section of the successfully manufactured NIR grating. Groove width: 322nm, depth: 890nm, grating period: 441nm. (Photo courtesy of IOF)

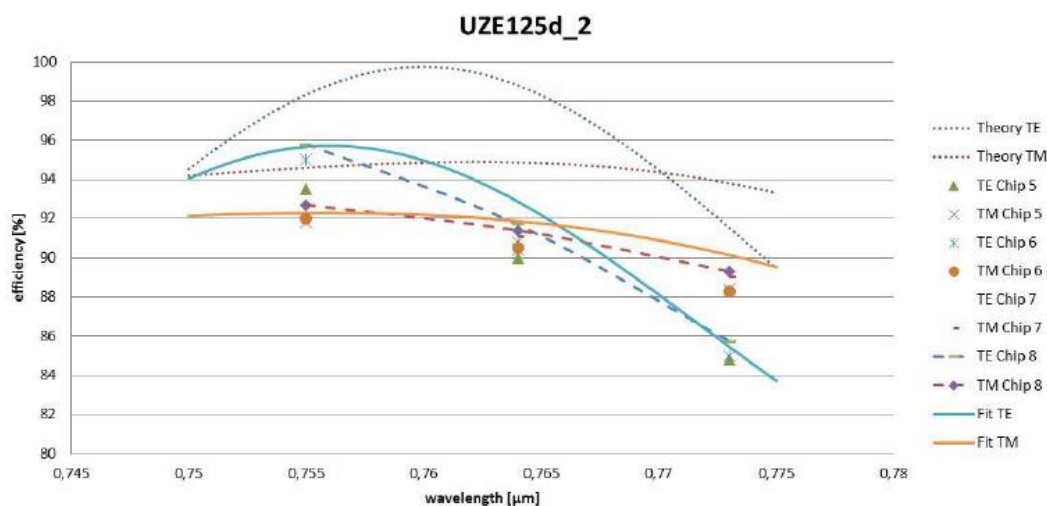


Fig. 17: Measured and simulated efficiencies of the NIR grating samples manufactured by IOF for Sentinel-5 of KT

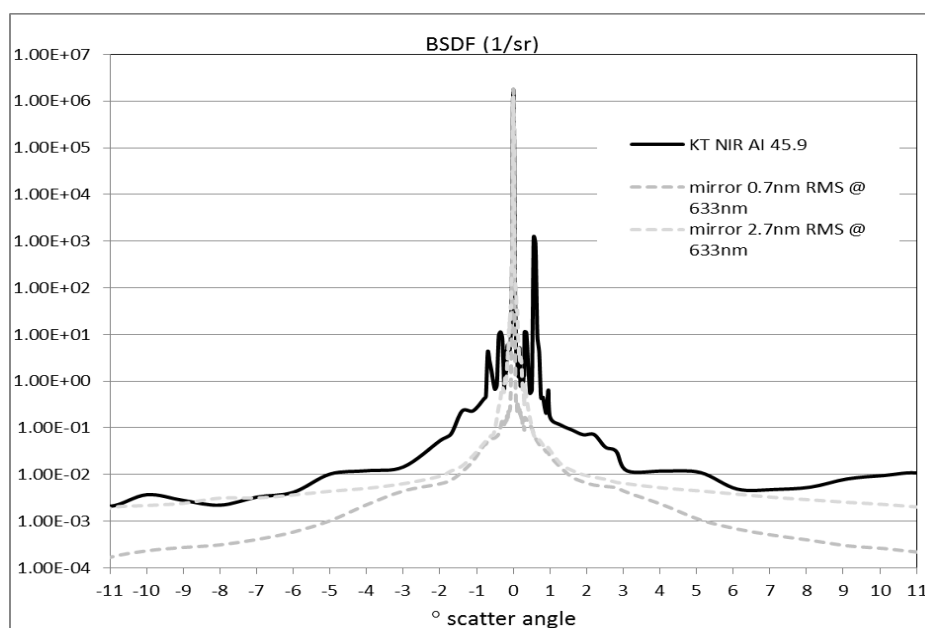


Fig. 18: BSDF at 633nm of the NIR grating of KT and two reference mirrors. The NIR grating is designed to operate in a wavelength range of 755nm to 773nm.

Grating pre-developments of ADS

The consortium around Airbus DS has initiated pre-developments for Sentinel-5 (see Table 3) of a replicated UV1 grating based on a technology of TNO and ZEISS and a binary transmission grating operating in the UV2-VIS with IOF. The UV1 grating (fig. 19) was manufactured with a silicon anisotropic wet etched silicon master. The idea behind this technology is to take advantage of the extremely smooth surfaces of the crystal planes of silicon wafers. These planes are brought to the surface using anisotropic wet etching. In order to have access to flawless crystal surfaces over long grooves the photoresist mask needs however to be perfectly parallel to those crystal planes. This is indeed a challenge and one of the reasons why it is very difficult to achieve an overall surface roughness equivalent to a flat super-polished wafer surface. The mask used in the frame of this pre-development was holographic. It was not considered as an optimal choice for a future flight grating but was used for cost reasons. After replication the grating was coated with aluminum. This grating underwent humidity and two cycles of thermal vacuum tests without serious changes in the optical response.

Tab. 3: Specifications of the pre-developed Sentinel-5 gratings (by ADS)

	Unit	S5-ADS-UV1 (TNO)	S5 ADS UV2VIS (IOF)
Grating type		Reflective blazed	binary transmission
Etch mask		replica from silicon anisotropic wet etch	e-beam lithographic
Wavelength range	nm	270-330	300-500
Used diffraction order	-	1	1
Line density	l/mm	2174	1500
Grating period	nm	460	667
Dent width	nm	NA (blazed ~19.5°)	354
Groove width	nm	NA (blazed ~19.5°)	313
Groove depth	nm	120	944
Trench aspect ratio width/depth		NA (wet etch)	3
Angle of incidence	deg	4	9.4 (in substrate)
Diffraction efficiency target		>65%	>55%
Polarisation sensitivity		< 20%	<15%
Substrate material		fused silica with polymer layer	fused silica
over-Coating		Aluminium	NA
Grating size	mm	50x60 mm ²	35x35 mm ²
Development status		Full size, manufactured	reduced size samples (30x30mm ²) manufactured
Qualification status		Passed humidity tests and 2 thermal vacuum cycles	-

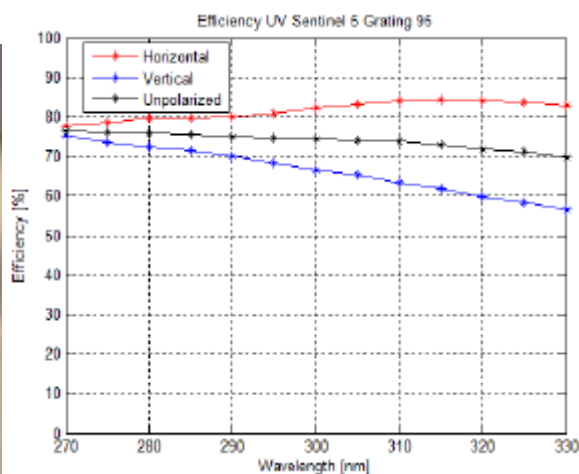


Fig. 19: Replicated UV1 grating sample and the measured efficiencies. (photo courtesy of TNO)

The stray light measurements made at ESA are shown in fig. 20. In the relevant scatter angular range above 1° this grating shows a stray light level below the reference mirror with a 2.7 nm RMS roughness. Assuming that in this scatter angular range the BSDF response scales with σ_m^2 an estimated UV1 mirror roughness of around 2 nm RMS is deduced. For scatter angles beyond 10° the BSDF response of the replicated mirror remains almost constant and becomes more important than the BSDF of the reference mirror. However, it can be safely assumed that with an optimized etch mask, a higher groove surface quality can be achieved and therefore a lower stray-light level expected for the future. It is noteworthy to mention that the BSDF of this UV1 grating is smooth and does not show any ghosts or oscillations as do the lithographic based manufactured gratings.

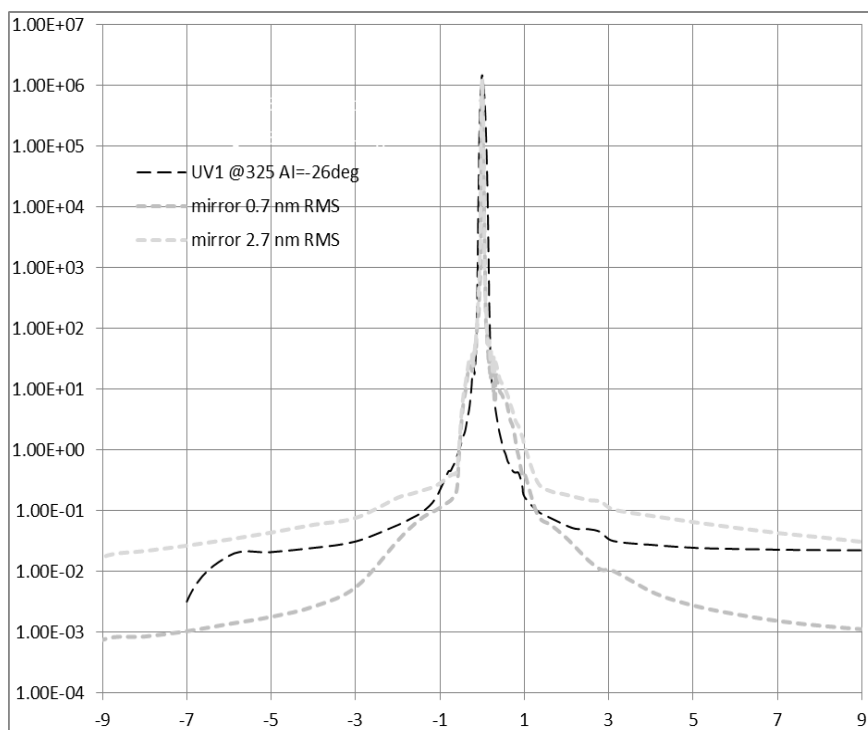


Fig. 20: BSDF of the UV1 grating at 325 nm which is in the operational wavelength range with the scaled BSDF of two reference mirrors.

The UV2VIS spectrometer design required a co-planar transmission grating covering the spectral range from 300nm up to 500nm. It is based on a binary profile with a groove aspect ratio of about 3 which can be considered as a low risk grating profile for the manufacturing (fig. 21). The theoretical and measured efficiencies are shown in fig. 22 and the stray light response in fig. 23. The BSDF of the grating up to a scatter angle of 2° follows the BSDF of the reference mirror with a roughness of 0.7 nm RMS, but shows in the same time clear oscillations with peaks which are at least an order of magnitude higher. For scatter angles greater than 2° the BSDF curve remains quite constant but remains for scatter angles up to 10° clearly below the response of the reference mirror with a roughness of 2.7 nm RMS. The oscillations are probably due to the lithographic e-beam mask patterning method.

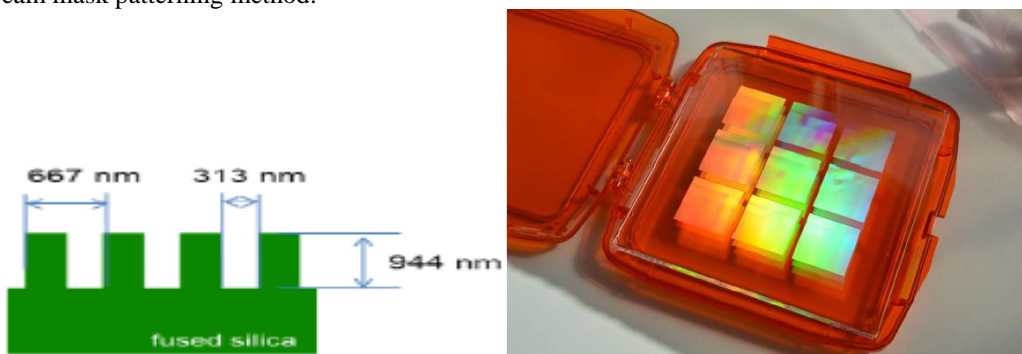


Fig. 21: On the left the UV2VIS grating profile is shown and on the right the final samples. (photo courtesy of IOF)

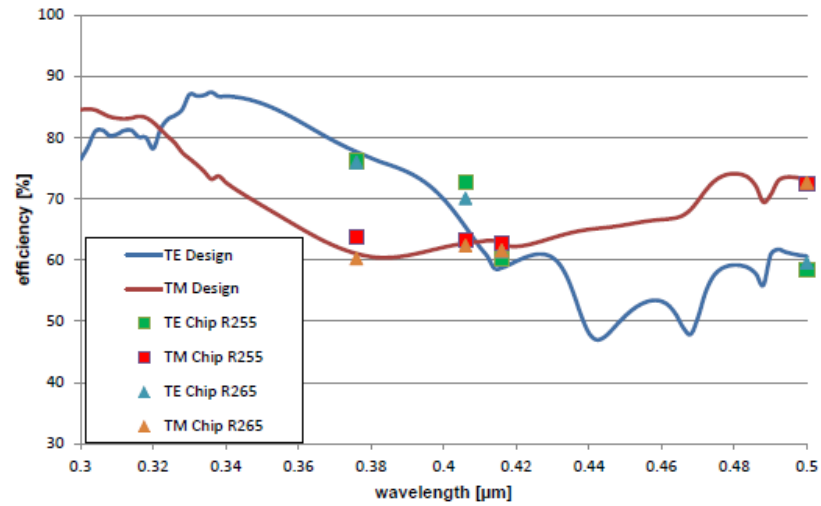


Fig. 22: Measured and simulated efficiencies of the Sentinel-5 UV2VIS grating of ADS

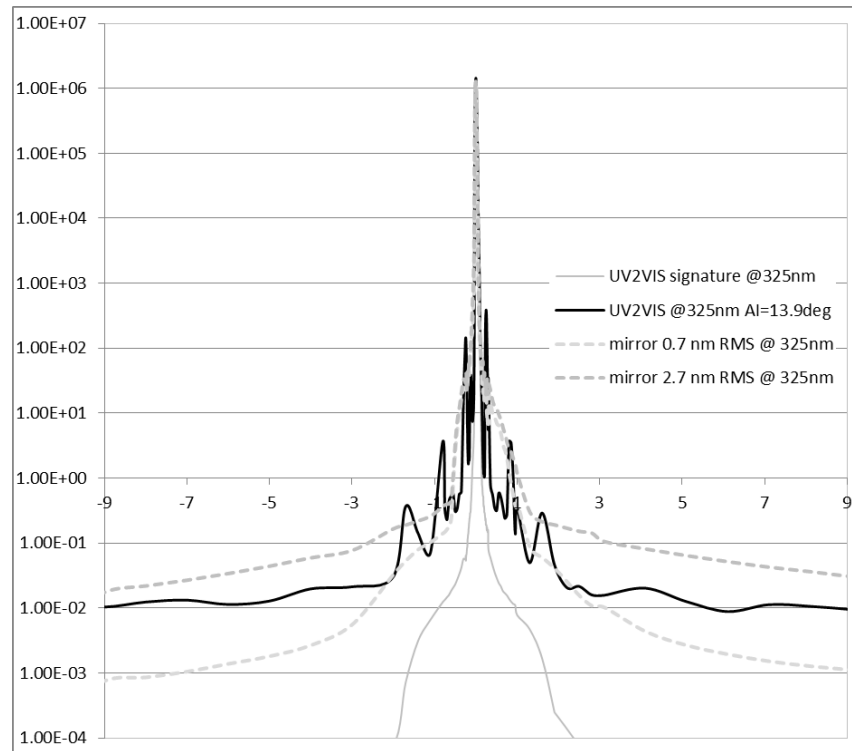


Fig. 23: BSDFs measured at 325 nm of the UV2VIS grating and two reference mirrors

The FLEX grating

FLEX is one of the two candidates ESA Earth Explorer 8 missions. The instrument features a high resolution NIR imaging spectrometer. Two instrument concepts are currently under feasibility studies, under the prime ship of Airbus Defense & Space France (ADS-F) and Thales Alenia Space France/Selex ES. One of the FLEX grating is in the pre-development phase at IOF and has a profile design (fig. 24) with a rather large aspect ratio of almost 7. The grating specifications are reported in Table 4 and straylight measurements of an early development have been published [6]. For this full size grating breadboard development IOF successfully took various measures to reduce the ghosts originating from the e-beam writing process. Fig. 25 shows BSDF measurements on samples before and after optimization of the ghosts' peaks. The improvement is clearly visible.

Tab. 4: The specifications of the pre-developed FLEX grating

	Unit	FIMAS
Grating type		binary, transmission
Wavelength range	Nm	677-800
Used diffraction order	-	+1
Line density	l/mm	1,499
Grating period	Nm	667
Dent width	Nm	430
Groove width	Nm	237
Groove depth	Nm	1639
Aspect ratio		6.9
Angle of incidence	deg	22° (in SiO ₂) 33° (in air)
Diffraction efficiency target		> 70% (G: > 90%)
Polarisation sensitivity		< 15% (G: < 2%)
Substrate material		fused silica
Grating size	mm	70 x 62 (elliptical)
Development status		Full size manufactured

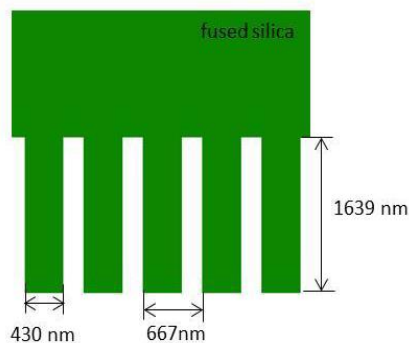


Fig. 24: The profile of one of the pre-developed FLEX grating

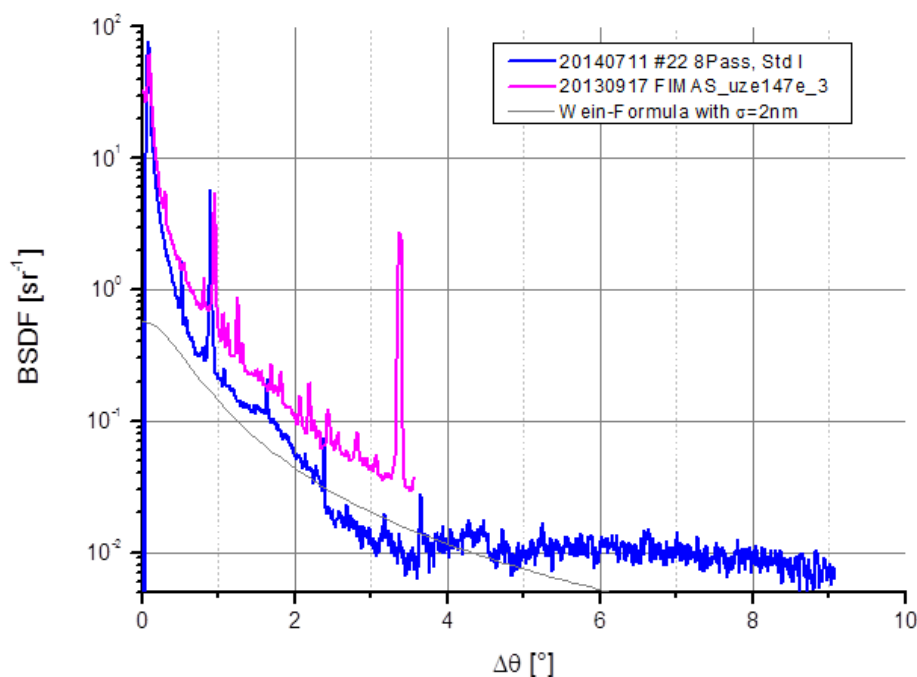


Fig 25: The blue curve is the BSDF of the latest (2014) FLEX grating sample showing well-damped ghosts. The magenta curve is the BSDF of an early development (2013) of the FLEX grating. For both BSDF the peak at 1 degree is a multiple reflection of the substrate. The BSDF value at 0 degree (diffraction order) is 51526 [1/sr].

4) CONCLUSIONS AND OUTLOOK

All the optical grating pre-developments made in the frame of recent ESA programs have been summarized and for some gratings the stray-light performances discussed. Compared to past missions, gratings with even higher efficiency, higher spectral resolution, lower stray light and lower polarization sensitivities are required. Another important parameter, critical for atmospheric chemistry missions, are the spectral features whose amplitude needs to be minimized.

The gratings manufactured by IOF are operating in transmission and are based on binary grating profile designs using e-beam lithography to produce the etch mask. The lithographic technique used to produce the grating profiles allows the design and manufacture of transmission gratings with low polarization sensitivities (<4%) combined with high diffraction efficiencies. Only one large spectral band (300-500nm) transmission grating had a higher polarization sensitivity (<10%). However, their measured BSDFs show clear side lobe peaks at scatter angles below 2°, close to the diffraction order, which are interpreted as ghosts generated by the e-beam writer. Techniques to attenuate the ghost amplitudes exist and are starting to be implemented successfully at IOF for the current grating developments.

The pre-developed reflective blazed gratings manufactured for the UV with holographic etch masks do not show ghosts. They have however quite a large polarization sensitivity (>15%). It must be noted that the high polarization sensitivity is not due to the use of holographic etch masks, but mostly due to their design based on a metallic reflective coating. Holographic etch masks can also be used to manufacture gratings operating in transmission.

To summarize the straylight behavior of the pre-developed gratings, the measured bsdf curves are below the measured straylight level of a reference mirror with a roughness of 2.7nm RMS but clearly higher than of one with a 0.7nm RMS roughness. This shows that the actual grating technology has still to be improved if roughness equivalent to a super polished surface had to be obtained. There seems therefore to be room for improvement for all grating technologies presented in this paper. For instance, the replicated UV grating from a wet etched silicon master has in theory the potential for clearly lower stray light levels since silicon crystal planes are the diffractive surfaces shaping the grating. A development effort in more optimized etch masks

might help improving the straylight performances. All other gratings, which were etched into fused silica, might with dedicated surface post processing (e.g. chemical etching) lower the roughness as well.

At instrument level a tendency towards spectrometer designs with immersed gratings is evident. This tendency is mainly driven by requirements on increased spectral resolution and the need for compactness. Actual designs are based on reflective immersed gratings or designs that attempt, with a grism plus prism (e.g. prism-grating-prism) arrangement, to achieve effective immersed gratings in transmission. Due to the fact that reflection within an immersed grating (today's typical immersed grating design) occurs in a high refractive index n_i medium (immersion material) the roughness of the σ_m immersed grating profile results theoretically in a higher TIS level:

$$\text{TIS}_{\text{immersed reflection}} \sim (2n_i\sigma_m/\lambda)^2 \quad (4)$$

For a silicon immersed grating surface in the SWIR for instance this translates into a TIS with an order of magnitude higher than for a reflective grating in air/vacuum for the same roughness. A silicon immersed grating in transmission, with vacuum in the grooves (and under the exaggerated assumption that all the light passes first from the immersion medium to vacuum and then back to the immersion medium again) has a theoretical TIS level four times lower than a reflective silicon immersed grating surface. For fused silica in the NIR for instance the TIS advantage of an immersed grating in transmission compared to the one operating in reflection would be 20, based on the same assumptions. It must be noted that the two prism surfaces traversed by the beam, the one before and one after the diffracting surface, also have to be accounted for to achieve an overall surface scatter figure of an immersed grating. In addition to shape the beam for the immersed grating, the prism(s) are also used to lower the optical aberrations in the spectrometer. Immersed gratings in transmission therefore offer the possibility to design relatively simple optical spectrometers compared to the immersed gratings in reflection. It also became visible that detailed models of scattered light for the reported gratings are missing. In particular for high aspect ratio grating profiles, where the surface roughness of the vertical side walls probably plays an important role, adequate straylight models would be very helpful.

ESA is at the moment initiating development activities for immersed gratings in transmission for the NIR (based on fused silica) and the SWIR (based on silicon) with the goal to obtain with minimal instrument sizes the high spectral resolutions and lower straylight levels required for future spectrometer missions.

5) ACKNOWLEDGMENTS

The authors would like to thank the grating manufacturers participating to the reported developments, namely Fraunhofer IOF and ZEISS in Jena, Horiba Jobin Yvon and TNO, as well as their industrial partners, Surrey Satellite Technology (SSTL), Airbus DS in Munich and Toulouse and Kayser-Threde in Munich. Particular thanks for the fruitful discussions and contributions are addressed in alphabetic order to Peter Bartsch (ADS), Torsten Diehl (ZEISS), Lars Erdmann (ZEISS), Dominic Doyle (ESA), Dominique Dubet (ADS), Juan Fernandez (SSTL), Dirk Kampf (KT), Jess Koehler (ADS), Audrey Liard (HJY), Gerald Mathe (ADS), Roman Windpassinger (KT) and Uwe Zeitner (IOF).

6) REFERENCES

- [1] Patrick W. Leech, Geoffrey K. Reeves, "Reactive ion etching of quartz and glasses for microfabrication", *Proc. SPIE* 3680, Design, Test, and Microfabrication of MEMS and MOEMS, 839 (March 10, 1999); doi:10.1117/12.341281.
- [2] E.-B. Kley, B. Schnabel, "E-beam lithography: a suitable technology for fabrication of high-accuracy 2D and 3D surface profiles", *Proc. SPIE* Vol. 2640, p. 71-80
- [3] U.D. Zeitner, D. Michaelis, E.-B. Kley, M. Erdmann, "High performance gratings for space applications," *Proc. SPIE* Vol. 7716, 77161K (2010).
- [4] Ruud W. M Hoogeveen, Rienk T. Jongma, Paul J. J. Tol, Annemieke Gloudemans, Ilse Aben, "Breadboarding activities of the TROPOMI-SWIR module", *Proceedings of the SPIE*, Volume 6744, pp. 67441T (2007).
- [5] www.breault.com/knowledge-base/scattering-asap
- [6] B. Harnisch, A. Deep, R. Vink, C. Coataniec, "Grating Scattering BRDF and Imaging Performances – A Test Survey performed in the frame of the FLEX Mission", ICSO 2012